ELSEVIER

Journal of Magnetism and Magnetic Materials 202 (1999) 62–68

Journal of magnetism and magnetic materials

www.elsevier.com/locate/jmmm

# Magnetic domain pinning in patterned perpendicular magnetic anisotropy material

Te-ho Wu[a,*], J.C. Wu[b], Bing-Mau Chen[c], Han-Ping D. Shieh[c]

[a]*Department of Humanities and Sciences, National Yunlin University of Science and Technology, Touliu, Taiwan 640, Taiwan, ROC*
[b]*Department of Physics, National Changhua University of Education, Changhua, Taiwan 500, Taiwan, ROC*
[c]*Institute of Electro-Optic Engineering, National Chiao-tung University, Hsinchu, Taiwan 300, Taiwan, ROC*

Received 6 October 1998; received in revised form 11 January 1999

**Abstract**

A method for pinning magnetic domains with prescribed shapes has been developed for the magneto-optical thin film material $Dy_x(FeCo)_{1-x}$. The pinning array of holes on the substrate was fabricated using electron beam lithography. The thin film of $Dy_x(FeCo)_{1-x}$ sandwiched between SiN layers was deposited onto a patterned polymethyl methacrylate layer. The pinned domains acquire the shape of the holes, while the sharpness of their boundaries depends on the size of the holes. The stability of the pinned domains is affected by the sample's magnetization. In our experiments, the minimum stable domain size pinned within the hole array was found to be around 50 nm in diameter. 

*PACS:* 75.70.Kw; 75.30.Gw; 75.50.Kj; 75.60.Ch

*Keywords:* Magneto-optical; Patterned substrate; Pinned magnetic domain; Electron-beam lithography; Domain stability

## 1. Introduction

In magneto-optical (MO) recording technology, studies of domain characteristics such as shape, size, stability, jaggedness, and wall width are important for the optimization of the media. Higher storage densities demand smaller stable domains and a reduced media noise. Observations have indicated that some of the media noise arises from domain irregularity, the rough magnetization transition regions, and a nonuniform distribution of magnetization within recorded domains [1–3]. Consequently, a written domain with a fixed shape and free from jaggedness could help in reducing media noise. One way to achieve this goal is by patterning of the disk substrates as was originally proposed in Ref. [4]. In this letter, we present a novel method for pinning the magnetic domains and discuss the relationships between the pattern geometry and the domain structure.

## 2. Experimental

Our method involves the confinement of domains within pre-formatted pinning sites, which are fabricated using electron-beam lithography. An

* Corresponding author. Tel.: +886-5-5342 601/3166; fax: +886-5342601/3166.
*E-mail address:* wuth@flame.yuntech.edu.tw (Te-ho Wu)

0304-8853/99/$ - see front matter 
PII: S0304-8853(99)00140-7

electron resist, polymethyl methacrylate (PMMA), was spun onto an SiN-coated Si-wafer and was baked at 140°C overnight. Arrays of square-, circle-, and star-shaped holes were created in the PMMA using a versatile pattern generator.[1] (The exposed PMMA was removed when placed in a 1 : 3 mixture of methyl isobutyl ketone (MIBK) and 2-propanol (IPA) for 80 s at 25°C and rinsed in IPA for 20 s, leaving square-, circle-, and star-shaped holes with 600 nm depth in PMMA.) The MO active layer – $Dy_x(FeCo)_{1-x}$ with 50 nm thickness was DC magnetron co-sputtered on the developed PMMA layer, and a 30 nm thick silicon nitride layer was subsequently deposited by RF magnetron reactive sputtering from an Si target in Ar and $N_2$ atmosphere to protect the MO layer. Fig. 1a is a SEM micrograph showing the MO/SiN sputter-coated trenches, which are made in the same batch as the hole array samples. The layer structure is: silicon/SiN (200 nm)/DyFeCo(50 nm)/SiN(30 nm) in the holes and silicon/SiN (200 nm)/PMMA(600 nm)/DyFeCo(50 nm)/SiN(30 nm) in the lands (see Fig. 1b). In this study, we used two compositions of rare-earth transition-metal amorphous magnetic film with perpendicular magnetic anisotropy: $Dy_{21.3}(Fe_{80}Co_{20})_{78.7}$ and $Dy_{27.3}(Fe_{80}Co_{20})_{72.7}$.

The sample's morphology and magnetic domain structure were observed by employing a magnetic force microscope (MFM). A Digital Instruments Nanoscope IIIa MFM, equipped with phase extender [5] was used in this study. The magnetic tip with a CoCr-coated Si tip magnetized along the tip axis was used to scan the magnetic domain structures in the tapping-lift mode [6]. Domain images represent the detected frequency shift of the vibrating cantilever. It has been shown that MFM contrast can be associated with up- and down-magnetized domains. Before the MFM measurements, the samples were either magnetized or demagnetized in magnetic fields perpendicular or parallel to the film plane [7,8]. During the perpendicular demagnetization process, a Polar Kerr microscope equipped with an electromagnet, having a maximum field capability of 5 kOe [9], was used to monitor the developing magnetic stripes and domains. For perpendicular magnetization and in-plane demagnetization, a 25 kOe field was used to saturate and to demagnetize the sample, respectively.

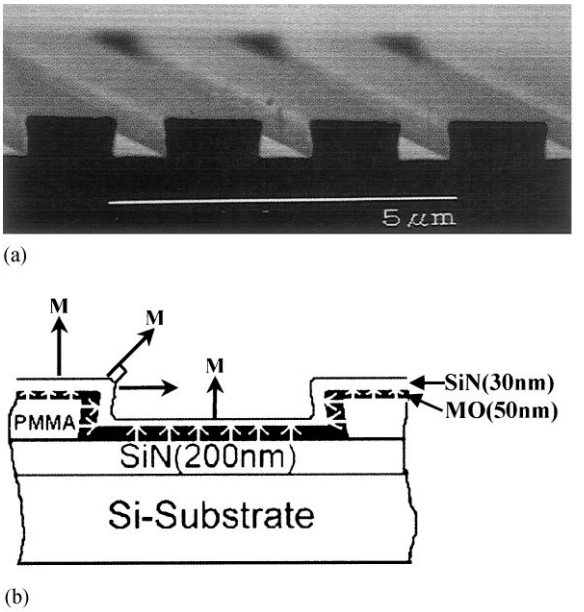


Fig. 1. (a) An SEM micrograph showing the cross sectional view of MO/SiN sputter-coated trenches, which are made in the same batch as the hole array samples. (b) Schematic diagram of the layer structure and the magnetization directions in (a).

## 3. Results and discussion

Magnetic domains were found to be pinned inside the hole arrays and resembled the geometric shapes of the holes. Shown in Fig. 2 are MFM images of patterned substrate hole arrays and magnetic domains in the $Dy_{21.3}(Fe_{80}Co_{20})_{78.7}$ sample. The left-hand side of Fig. 2a displays the patterned hole array morphology, while the right-hand side displays pinned magnetic domains within the square hole arrays after applying a 25 kOe magnetic field. Fig. 2b displays a three-dimensional magnified view of the pinned magnetic domains. In

[1] A 30 kV of Hitachi S2460N SEM equipped with a versatile pattern generator is used for the structure fabrication in this study. The writing software, Nanopattern Generator Systems (NPGS), is produced by JC Nabity Lithography Systems, Bozeman, MT59717.

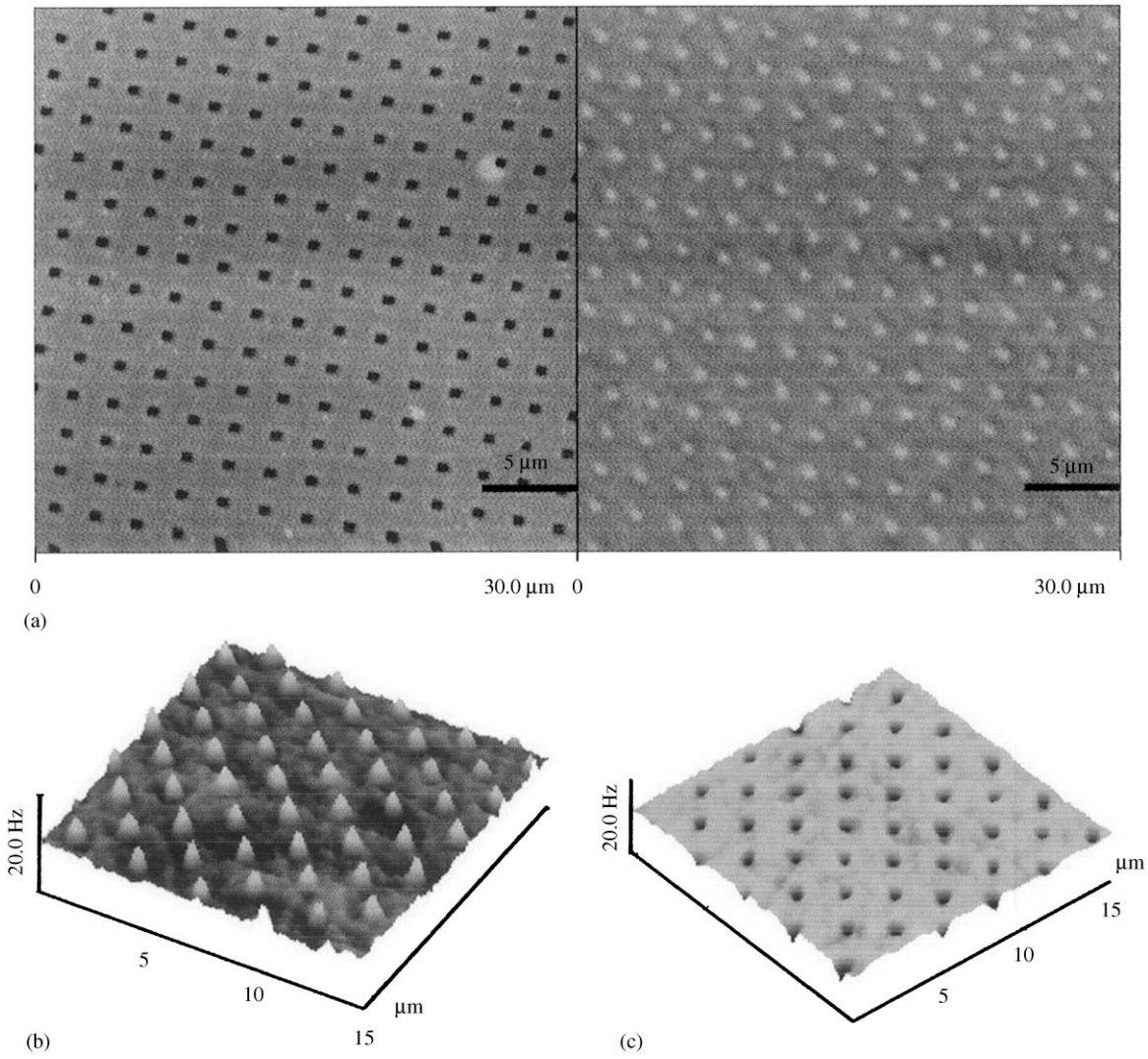


Fig. 2. (a) The left-hand side displays the patterned substrate morphology, while the right-hand side displays the pinned magnetic domain pattern. (b) The three-dimensional magnified view of (a) of the pinned magnetic domain. (c) The reversed pinned domains of (b).

order to verify that the frequency shift of Fig. 2b interprets the magnetic signal, we apply an opposite magnetic field, −25 kOe, to switch the magnetic moment. As shown in Fig. 2c, the pinned domains are all reversed. Thus, the frequency shift of Fig. 2b indeed reveals the magnetic domains.

By using e-beam lithography, we can make most of the desired geometry hole arrays. Fig. 3a shows a pattern of a circle-shaped (with 1 μm in diameter) pinning domain and Fig. 3b displays another pattern of a star-shaped (with 1.5 μm in diameter) pinning domain in the $Dy_{27.3}(Fe_{80}Co_{20})_{72.7}$ sample. Fig. 3a was taken after applying a magnetic field perpendicular to the film plane, while Fig. 3b was taken as deposited, i.e. without any externally applied magnetic field.

The pinning mechanism is believed to be a vector combination of both perpendicular magnetization

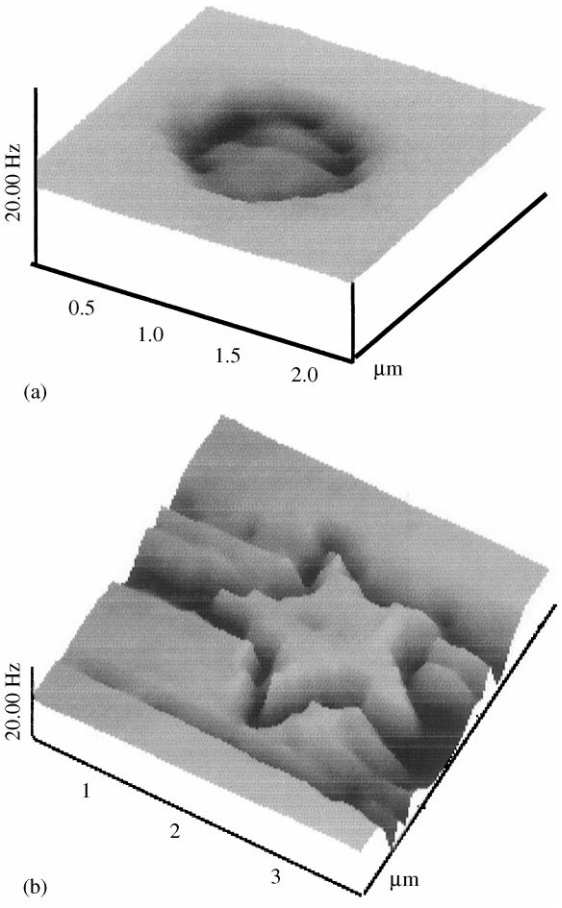


Fig. 3. MFM images of the pinned domains within (a) a circular hole and (b) a star-shaped hole.

on the side walls and in the bottom areas of the hole. Since the samples we have studied possess perpendicular anisotropy, the magnetization direction on every side wall is almost perpendicular to the magnetization at the bottom. The magnetization near the rim of the hole, instead of being perpendicular, is inclined towards the surface acting as a transition region and causing the pinning effect. The evidence can be seen in the SEM image of Fig. 1a, which indicates the existence of MO material covering every region of the sample, including top plate, rim, side walls and bottom area. Fig. 1b schematically displays the layer structure and the magnetization directions in the sample of Fig. 1a.

Pinning by the vector combination effect also manifests itself in the fact that the domain shape depends on the hole size. Fig. 4 shows that for larger holes the square shape of the domain is sharper. The size of the four domains in Fig. 4a is $0.5\ \mu m \times 0.5\ \mu m$ square, while the size in Fig. 4b is $1\ \mu m \times 1\ \mu m$ square. For larger holes, the vector effect of the side walls is overcome by the larger total magnetic moment produced in the bottom area; consequently, the domain has a sharper square shape.

That the magnetization affects the domain sharpness can be further verified by examining the

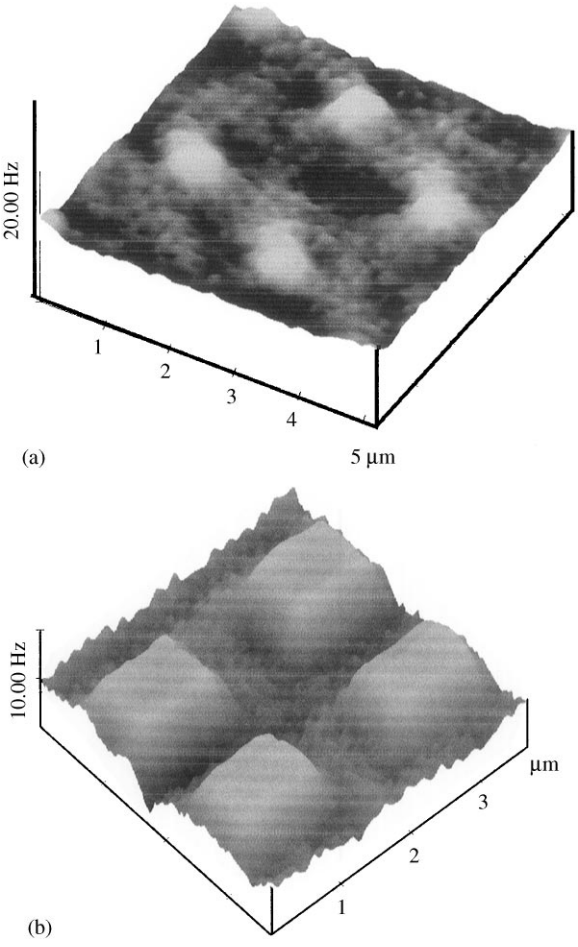


Fig. 4. MFM images show that for larger holes the square shape of the domain is sharper, (a) $0.5\ \mu m \times 0.5\ \mu m$ and (b) $1.0\ \mu m \times 1.0\ \mu m$ square holes.

sample's magnetization influence on the domain stability, as shown in Fig. 5. Before comparing the differences between the images of Fig. 5a and Fig. 5b, we describe the way in which these images were produced. The sample's magnetization was first saturated in one direction, say along the easy axis, by applying a magnetic field far greater than the sample's coercivity. The applied field was then increased in the reverse direction and allowed to approach near the coercivity until it caused domain wall motion. The wall motion was monitored using a Kerr microscope. By the time the wall reached near the center of the patterned area, the applied magnetic field was turned off to ensure that the magnetic domains were developed. The sample was then moved to the MFM for image acquisition. Fig. 5a is a three-dimensional view of an MFM image with well-defined magnetic domains for a $Dy_{27.3}(Fe_{80}Co_{20})_{72.7}$ sample. The upper left part of the image represents the saturated magnetic moments before reversing the applied field, on the other hand, the lower right part of the image

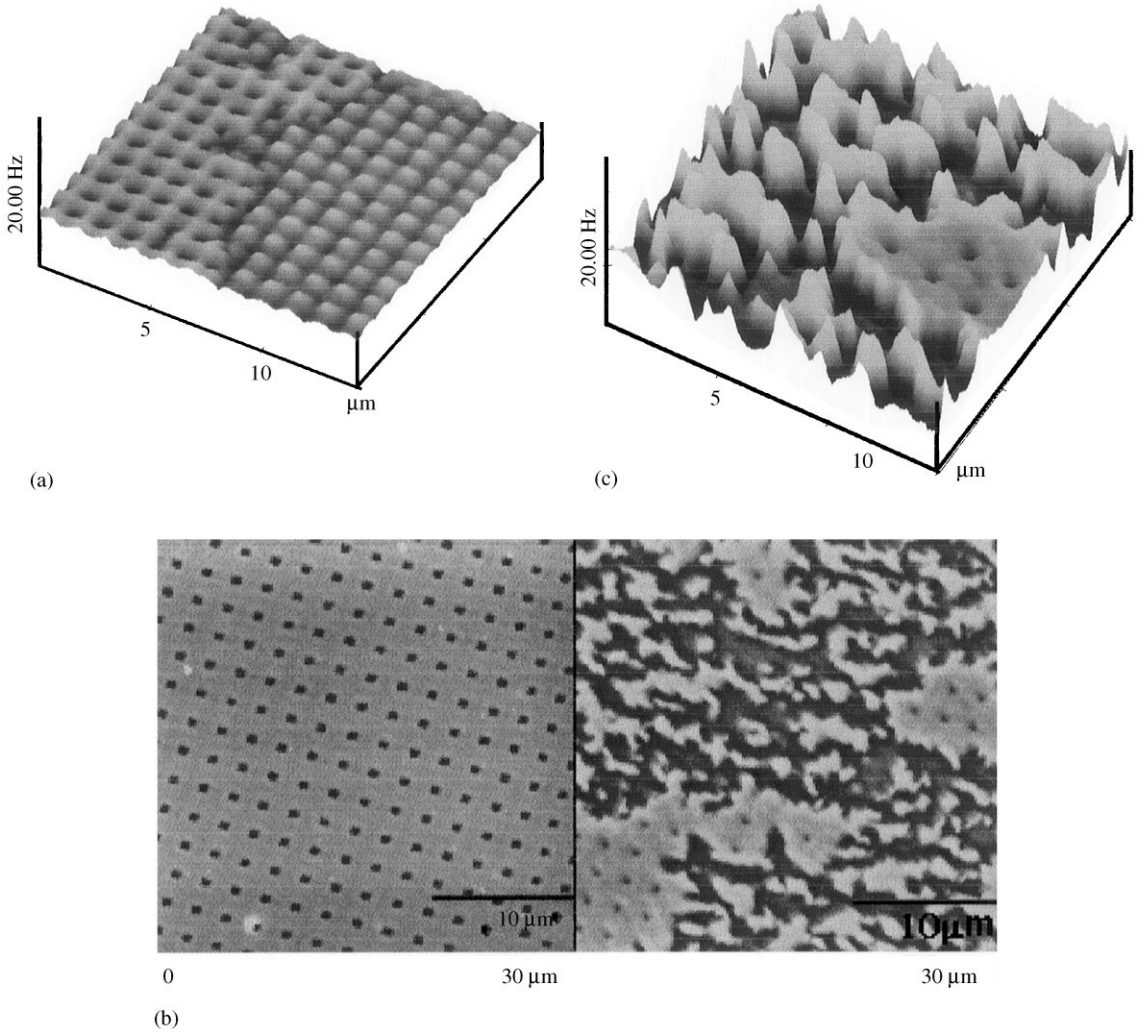


Fig. 5. (a) An MFM image of the sample containing $Dy_{27.3}(Fe_{80}Co_{20})_{72.7}$ showing that domains are confined inside the holes. (b) Hole morphology (left) and magnetic domain image (right) in the $Dy_{21.3}(Fe_{80}Co_{20})_{78.7}$ sample. (c) A three-dimensional magnified view of (b), as the arrow indicates.

represents opposite magnetic moments after reversing the applied field causing the domain wall to move through. Fig. 5b displays a hole array morphology (left) and magnetic domain image (right) for a $Dy_{21.3}(Fe_{80}Co_{20})_{78.7}$ sample. Fig. 5c is a three-dimensional magnified view of Fig. 5b, as the arrow indicates. On the right-hand side of Fig. 5b, the magnetic domain pattern exhibits a result that is quite different from that of Fig. 5a: the previously saturated domains disappear in areas where the domain wall moves across after reversing the applied field. In other words, the domain stability in the $Dy_{21.3}(Fe_{80}Co_{20})_{78.7}$ sample is weaker than that in the $Dy_{27.3}(Fe_{80}Co_{20})_{72.7}$ sample. This can be seen clearer from the three-dimensional view of the domain image. The results can be explained by comparing the two samples' saturation magnetization ($M_s$) measured by vibrating sample magnetometry (VSM). The $Dy_{21.3}(Fe_{80}Co_{20})_{78.7}$ sample possesses a larger $M_s$ (150 emu/cc) and a lower coercivity ($H_c = 1.62$ kOe) when compared with the $Dy_{27.3}(Fe_{80}Co_{20})_{72.7}$ sample which has $M_s = 75$ emu/cc and $H_c = 2.70$ kOe). Thus, the demagnetization field ($4\pi M_s = 1.88$ kOe) of the $Dy_{21.3}(Fe_{80}Co_{20})_{78.7}$ sample is large enough to demagnetize the local area when the domain wall moves through. In contrast, the coercivity of the $Dy_{27.3}(Fe_{80}Co_{20})_{72.7}$ sample is larger than its demagnetization field ($4\pi M_s = 0.94$ kOe), so it maintains the stability of the pinned domains. In addition, the larger $M_s$ of the $Dy_{21.3}(Fe_{80}Co_{20})_{78.7}$ sample could be further verified by comparing the sample's magnetic force on the probing tip of MFM. The larger the sample magnetization, the greater the force gradient that is exerted on the tip, and this is manifested in the modulation depth of the measured image (see Fig. 5c). Apparently, the image depth (frequency shift) of Fig. 5c is greater than that of Fig. 5a. We conclude that the sample's saturation magnetization dictates the stability of the confined domains.

When the applied magnetic field was increased to reverse the magnetization, we found that the coercivity was higher within the patterned region when compared with that outside the patterned area [4,10]; for instance, for the square hole arrays domain wall motion coercivity outside the patterned area for sample $Dy_{27.3}(Fe_{80}Co_{20})_{72.7}$ is

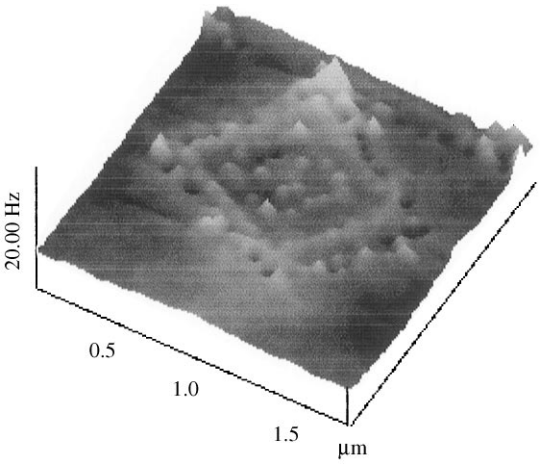


Fig. 6. Concentric magnetic domain pattern; the minimum stable domain found in this image is about 50 nm in diameter.

2.7 kOe, while inside the patterned area, the coercivity is 3.9 kOe. It seems that the magnitude of the coercivity of the hole arrays also depends on the hole geometry. In the present study, the local coercivity of the square holes was generally found to be higher than those in the circle- and star-shaped holes. We will report the quantitative results of this study in a separate publication.

Finally, we found that a concentric domain pattern could be formed in a single pinning hole if the hole possesses some particular shapes, for example, triangular [11]. In addition, smaller stable domains could be created on the boundary of the concentric rings, as shown in Fig. 6. The smallest stable domain found in this image is about 50 nm in diameter.

## 4. Conclusions

A technique has been developed for pinning the magnetic domains in thin film MO materials within hole arrays with square, circle, and star shapes. It is possible to fabricate any desired domain geometry with this technique. However, for smaller domains, the present results indicate that the ratio of hole diameter to depth is critical. It was observed that the stability of the pinned domain is affected by the sample's magnetization. Further investigation is necessary to understand the effect of changing the ratio of hole diameter to depth and the sample's

magnetization on the stability of domains with small size and definite shape in thin film MO materials.

## Acknowledgements

We are grateful to Professor M. Mansuripur of the University of Arizona in Tucson for stimulating discussions and for his comments on a preprint of this article. This work is supported by the National Science Council, the Republic of China, under Contract No. NSC 87-2112-M-224-001.

## References

[1] Te-ho Wu, M. Mansuripur, Proc. of MORIS'92, J. Magn. Soc. Japan 17 S1 (1993) 131.
[2] Y. Honda, N. Inaba, F. Tomiyama, T. Yamamoto, M. Futamoto, Jpn. J. Appl. Phys. 34 (1995) L987.
[3] C.-J. Lin, D. Rugar, IEEE Trans. Magn. MAG-24 (1988) 2311.
[4] S. Gadetsky, T. Suzuki, J.K. Erwin, M. Mansuripur, Proc. of MORIS'94, J. Magn. Soc. Japan, 19 S1 (1995) 91.
[5] K. Babcock, M. Dugas, S. Manalis, V. Elings, Mater. Res. Soc. Symp. Proc. 355 (1995) 311.
[6] K. Babcock, V.B. Elings, J. Shi, D.D. Awschalom, M. Dugas, Appl. Phys. Lett. 69 (1996) 705.
[7] Te-ho Wu, J. Appl. Phys. 81 (1997) 5321.
[8] M. Hehn, K. Ounadjela, J.-P. Bucher, F. Rousseaux, D. Decanini, B. Bartenlian, C. Chappert, Science 272 (1996) 1782.
[9] B.E. Bernacki, M. Mansuripur, J. Appl. Phys. 69 (1991) 4960.
[10] J.A. Barnard, H. Fujiwara, V.R. Inturi, J.D. Jarrat, T.W. Scharf, Appl. Phys. Lett. 69 (1996) 2758.
[11] Te-ho Wu, J.C. Wu, Bing-Mau Chen, Han-Ping D. Shieh, IEEE Trans. Magn. 34 (1998) 1994.